THE ASTROPHYSICAL JOURNAL, 668:1103–1108, 2007 October 20
Preprint typeset using LaTeX style emulateapj v. 10/09/06

FLAME-DRIVEN DEFLAGRATION-TO-DETONATION TRANSITIONS IN TYPE IA SUPERNOVAE?

F. K. RÖPKE[1]
Max-Planck-Institut für Astrophysik, Karl-Schwarzschild-Str. 1, D-85741 Garching, Germany
Draft version September 26, 2007

ABSTRACT

Although delayed detonation models of thermonuclear explosions of white dwarfs seem promising for reproducing Type Ia supernovae, the transition of the flame propagation mode from subsonic deflagration to supersonic detonation remains hypothetical. A potential instant for this transition to occur is the onset of the distributed burning regime, i.e. the moment when turbulence first affects the internal flame structure. Some studies of the burning microphysics indicate that a deflagration-to-detonation transition may be possible here, provided the turbulent intensities are strong enough. Consequently, the magnitude of turbulent velocity fluctuations generated by the deflagration flame is analyzed at the onset of the distributed burning regime in several three-dimensional simulations of deflagrations in thermonuclear supernovae. It is shown that the corresponding probability density functions fall off towards high turbulent velocity fluctuations much more slowly than a Gaussian distribution. Thus, values claimed to be necessary for triggering a detonation are likely to be found in sufficiently large patches of the flame. Although the microphysical evolution of the burning is not followed and a successful deflagration-to-detonation transition cannot be guaranteed from simulations presented here, the results still indicate that such events may be possible in Type Ia supernova explosions.

Subject headings: Stars: supernovae: general – Hydrodynamics – Instabilities – Turbulence – Methods: numerical

1. INTRODUCTION

The question of whether deflagration-to-detonation transitions (DDTs) may occur in type Ia supernova (SN Ia) explosions has been a puzzle since the scenario of delayed detonations was suggested in the first place (Khokhlov 1991). If a supersonic detonation burning mode occurs at all in SNe Ia, such a transition is inevitable because a prompt detonation fails to produce the observed intermediate mass elements (Arnett 1969). For these to be synthesized, burning must partially take place at low fuel densities. A pre-expansion of the white dwarf (WD) material before burning is only possible for subsonic propagation of the thermonuclear flame. Consequently, the standard picture is that of an accreting WD which getting close to the Chandrasekhar limit becomes unstable to a thermonuclear runaway and ignites a subsonic deflagration flame. In contrast to the shock-driven detonation, flame propagation is mediated by microphysical transport in this mode. However, this scenario is intricate because the energy released in burning may expand the WD so rapidly, that the slow flame is not capable of burning sufficient amounts of material before it has dropped to densities at which burning cannot be sustained any longer. This way, the explosion would be far too weak to be consistent with observations. Therefore, the flame needs to accelerate and two possible mechanisms for this have been suggested.

The first is well-founded on known physical principles and is based on the fact that the buoyant rise of the burning bubbles generates strong turbulent motions due to Rayleigh-Taylor and Kelvin-Helmholtz instabilities. The flame interacts with eddies of the resulting turbulent cascade and, by means of surface area increase, accelerates significantly. This turbulent deflagration scenario has been recently studied in detail in three-dimensional simulations (e.g. Reinecke et al. 2002b; Gamezo et al. 2003; Röpke & Hillebrandt 2005). It has been shown that it may lead to explosions of the WD star meeting the gross properties of observed SNe Ia (Röpke et al. 2007a). However, some issues remain unsolved in this model. First, in its current implementations it can explain only the weaker events. Second, it may in some configurations leave behind unburnt material in the central parts of the ejecta, which disagrees with observations (Kozma et al. 2005). Third, it has problems explaining the high-velocity intermediate mass elements seen in the spectra of SNe Ia.

These weaknesses of the models may possibly be cured if a second way of flame acceleration, a DDT, takes place in later stages of the explosion. One-dimensional parameterizations of this "delayed detonation model" showed best agreement with observations assuming this transition to occur once the fuel density ahead of the flame has dropped to $\sim 10^7\,\mathrm{g\,cm^{-3}}$. Unfortunately, such a transition is hypothetical as of yet, since no convincing mechanism has been identified that would work robustly in a SN Ia.

Niemeyer & Woosley (1997) pointed out that the only fundamental change in the flame properties is found at the transition from the flamelet regime of turbulent combustion to the distributed regime. In the first, which holds for most parts of the explosion process, the interaction of the flame with turbulence is purely kinematic. The flame front as a whole is corrugated by turbulent eddies, but its internal structure remains unaffected. At a first glance this seems surprising, since Reynolds numbers $Re(L)$ at scales of $L = 10^7$ cm typical for the situation in SNe Ia are of the order of 10^{14}. The corresponding Kolmogorov scale, $\eta \sim L\,[Re(L)]^{-3/4}$, down to which the turbulent cascade extends, is $\sim 10^{-4}$ cm—much smaller than the flame thickness. However, assuming Kolmogorov scaling, the velocity fluctuations (denoted as v' in the following) decrease with the cubic root of the length scale under consideration within the inertial range of the turbulent cascade. This constitutes the so-called Gibson scale, at which the laminar flame speed is comparable to v'. Below the Gibson scale, the flame burns through turbulent eddies faster

[1] Also at: Department of Astronomy and Astrophysics, University of California Santa Cruz, 1156 High Street, Santa Cruz, CA 95064, U.S.A.

TABLE 1
PARAMETERS OF THE THREE-DIMENSIONAL DEFLAGRATION SN IA SIMULATIONS USED FOR THE ANALYSIS.

name	spatial coverage	resolution (computational grid cells per dimension)	central density [10^9 g cm^{-3}]
Simulation I	full star	1024	2.9
Simulation II	full star	640	2.0
Simulation III	octant	256	2.9

than they can deform it, and therefore they do not affect the flame shape considerably. However, since the laminar burning velocity and the flame thickness depend on the fuel density (Timmes & Woosley 1992), the Gibson scale decreases in the course of the explosion while the flame structure becomes wider. Therefore, turbulent eddies will eventually penetrate the internal flame structure and mix heated material, fuel, and ashes.

It turns out that this onset of the distributed burning regime takes place at fuel densities favored for DDTs in one-dimensional simulations (Niemeyer & Woosley 1997). Studying the microphysics of burning in this regime, Lisewski et al. (2000) concluded that triggering a detonation may be possible for sufficiently strong turbulence. The velocity fluctuations should be close to 10^8 cm s^{-1} (corresponding to $\sim$20% sound speed), but at this time the available two-dimensional supernova simulations seemed to exclude such high turbulent velocities. A re-analysis of this scenario is underway (Woosley 2007) and arrives at similar conclusions. If a mechanism providing a deflagration-to-detonation transition driven by the flame itself existed, the parameter deciding on triggering a detonation would be the strength of the mixing of the flame structure, which is determined by the magnitude of v'. This value can be estimated from three-dimensional numerical simulations of the deflagration stage of the explosion and is the focus of the present paper.

2. APPROACH

To determine v', data from several three-dimensional simulations of the deflagration stage in thermonuclear supernovae are analyzed. These simulations apply the methods described in detail by Reinecke et al. (1999, 2002a), Röpke (2005), and Schmidt et al. (2006). The key features include flame tracking via a level-set approach, a turbulent subgrid-scale model, and a moving computational grid to follow the expansion of the WD.

Simulation I (Röpke et al. 2007a) was carried out on 1024^3 grid cells and comprised the full star, as did simulation II which was set up on 640^3 grid cells. Only an octant of the WD was accounted for in Simulation III with a 256^3 cells grid assuming mirror symmetry with the other octants. The exploding WD had an initial central density of 2.9×10^9 g cm^{-3} in simulations I and III, while for simulation II a central density of 2.0×10^9 g cm^{-3} was chosen. These parameters of the setup are summarized in Table 1. All initial WD configurations were composed of a mixture of equal parts, by mass, of carbon and oxygen. The flame was ignited in multiple kernels spherically distributed around the center of the star and partially overlapping, similar to the scenarios presented by Röpke et al. (2006).

The quantity under consideration here is v' experienced by the flame in the distributed burning regime. Of course, this is

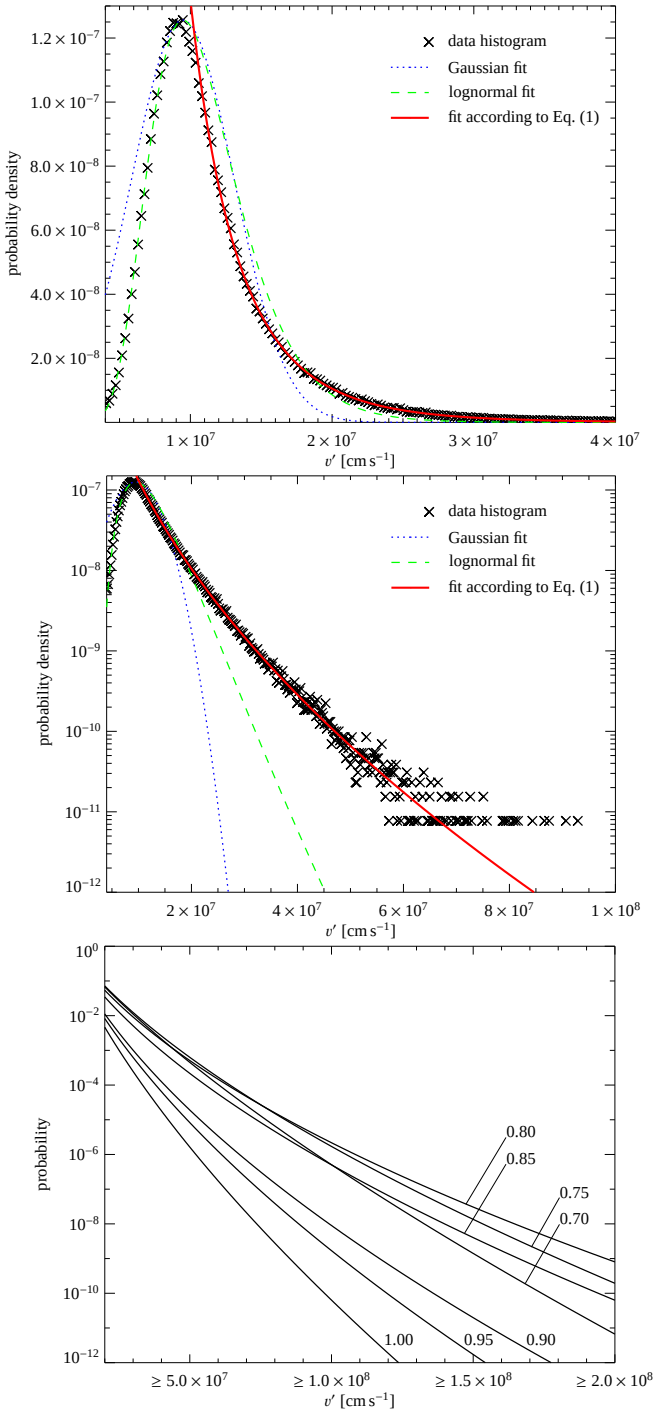

FIG. 1.— Fits to the histogram of v' in simulation I at t = 0.80 s for $1 < \rho[10^7\,\mathrm{g\,cm^{-3}}] \leq 3$ *(top two panels)*, and the probability of finding v' larger than a given value according to eq. (2) for different times in the same density interval *(bottom panel)*.

not directly resolvable in simulations carried out on the scales of the WD star. Therefore, an estimate of the turbulent velocities at the flame is obtained from the subgrid-scale turbulence model. It provides the value of v' at the scale of the computational grid. Since the size of the grid cells is a dynamical quantity in the implementation, it is rescaled to a length scale of 10^6 cm for comparison. To this end, a Kolmogorov spectrum was assumed, which need not necessarily apply to the actual scaling of turbulence at the considered spatial range; however, in the simulations presented by Zingale et al. (2005)

TABLE 2
MAXIMUM TURBULENT VELOCITIES AT A SCALE OF 10^6 cm, FIT PARAMETERS ACCORDING TO EQ. (1), PROBABILITY OF FINDING $v' \geq 10^8\,\mathrm{cm\,s^{-1}}$ ($P(10^8)$), ESTIMATED FLAME AREA A_{est}, SIZE OF THE PATCH OF THE FLAME WHERE $v' \geq 10^8\,\mathrm{cm\,s^{-1}}$ ($A_{\mathrm{est}}P(10^8)$), AND NUMBER OF COMPUTATIONAL CELLS TAKEN INTO ACCOUNT IN THE ANALYSIS FOR SIMULATION I IN THE DENSITY RANGE $1 < \rho[10^7\,\mathrm{g\,cm^{-3}}] \leq 3$.

t [s]	$v'_{\mathrm{max}}(10^6\,\mathrm{cm})$ $[10^7\,\mathrm{cm\,s^{-}1}]$	$-a_0$ $[10^{-4}]$	a_1 $[10^{-1}]$	$-a_2$	$P(10^8)$	A_{est} [cm^2]	$A_{\mathrm{est}}P(10^8)$ [cm^2]	cells
0.70	6.70	0.356691 ± 0.0004	7.12569 ± 0.0006	12.4931 ± 0.007	$5.062E-07$	$7.85E+16$	$3.98E+10$	55,341
0.75	8.38	2.97325 ± 0.006	5.98318 ± 0.001	11.1650 ± 0.02	$1.702E-06$	$5.35E+17$	$9.11E+11$	274,015
0.80	11.5	15.3360 ± 0.010	5.12493 ± 0.0004	9.90905 ± 0.007	$2.179E-06$	$1.50E+18$	$3.28E+12$	574,769
0.85	10.1	8.92170 ± 0.02	5.44507 ± 0.001	10.3121 ± 0.02	$5.016E-07$	$2.52E+18$	$1.27E+12$	736,593
0.90	7.05	8.92137 ± 0.006	5.55688 ± 0.0004	9.47029 ± 0.007	$8.966E-09$	$2.98E+18$	$2.67E+10$	614,195
0.95	6.20	5.18888 ± 0.01	5.87899 ± 0.001	9.71264 ± 0.02	$1.691E-09$	$2.89E+18$	$4.89E+09$	443,823
1.00	4.24	2.20126 ± 0.005	6.39985 ± 0.001	9.98804 ± 0.02	$6.351E-11$	$2.28E+18$	$1.45E+08$	263,740

TABLE 3
SELECTED PARAMETERS FOR DIFFERENT DENSITY INTERVALS AND SIMULATIONS. THE NOTATION IS THE SAME AS IN TABLE 2.

t [s]	$v'_{\mathrm{max}}(10^6\,\mathrm{cm})$ $[10^7\,\mathrm{cm\,s^{-1}}]$	$A_{\mathrm{est}}P(10^8)$ [cm^2]	cells
Simulation I, $1 < \rho[10^7\,\mathrm{g\,cm^{-3}}] \leq 2$			
0.70	5.37	$6.72E+05$	5723
0.75	7.47	$1.05E+11$	80,438
0.80	11.5	$1.66E+12$	276,683
0.85	10.1	$1.20E+12$	443,841
0.90	6.63	$1.82E+10$	423,654
0.95	6.20	$9.74E+09$	355,975
1.00	4.24	$2.58E+08$	243,480
Simulation I, $2 < \rho[10^7\,\mathrm{g\,cm^{-3}}] \leq 3$			
0.70	6.70	$6.00E+10$	49,618
0.75	8.38	$4.40E+11$	193,577
0.80	9.30	$9.83E+11$	298,086
0.85	7.79	$3.06E+11$	292,752
0.90	7.05	$1.78E+09$	190,541
0.95	4.81	$6.96E+08$	87,848
1.00	3.22	$4.92E+07$	20,260
Simulation II, $1 < \rho[10^7\,\mathrm{g\,cm^{-3}}] \leq 3$			
0.75	5.27	$4.52E+10$	8312
0.80	6.65	$1.95E+11$	45,902
0.85	8.36	$8.37E+10$	121,638
0.90	8.46	$1.37E+11$	200,764
0.95	7.02	$1.80E+11$	239,816
1.00	6.65	$6.70E+10$	230,245
1.05	5.79	$2.91E+11$	187,809
1.10	5.18	$3.38E+11$	139,548
1.15	4.45	$1.67E+10$	90,103
Simulation III, $1 < \rho[10^7\,\mathrm{g\,cm^{-3}}] \leq 3$			
0.75	5.18	$5.11E+12$	9865
0.80	5.67	$6.17E+10$	15,073
0.85	6.51	$1.39E+12$	18,209
0.90	5.75	$3.80E+12$	17,166
0.95	4.04	$2.61E+11$	12,589
1.00	3.00	$2.10E+08$	8098

and Röpke et al. (2007a). Kolmogorov turbulence is indeed recovered for buoyancy-unstable flames. In any case, the potential error introduced by this procedure is expected to be small, since the grid scales at times examined here will not deviate significantly from 10^6 cm. Another simplification is introduced by reducing the data sets by a factor of 2 in each direction, leaving out every second cell of the computational grid. Although this deteriorates the statistics, it simplifies the analysis of the large data sets from the highly resolved simulations. The distributed burning regime is expected to be reached for fuel densities in the range $1\ldots3\times10^7\,\mathrm{g\,cm^{-3}}$ (Woosley 2007; Niemeyer & Kerstein 1997). Therefore, we measure v' determined by the subgrid-scale model in computational grid cells cut by the flame front in this density range. This introduces two uncertainties. First, these cells contain mixed states of fuel and ashes. Consequently, the values we obtain are not equal (but, due to the small density jump over the flame, similar to) the values in pure fuel. Although it may seem compelling to restrict the analysis to cells sufficiently far away from the flame so that they contain pure fuel, this would require a distance of at least three cells, and turbulence will be considerably weaker that far ahead of the flame. Values derived this way would therefore not well represent the v' experienced by the flame front. Second, as we are looking for maxima of v', the subgrid-scale model will provide only a mean value on the size of the grid cells. Of course, there will be a maximum of this quantity, which will be determined in the following, but due to the intermittent nature of turbulence, rare extrema exceeding these values are possible on smaller scales in the real situation.

3. RESULTS AND IMPLICATIONS

The following discussion focuses on simulation I (the corresponding values are given in Tables 2 and 3). Results from the other simulations are included in Table 3 and corroborate the generality of these results. The possibility of triggering a detonation at a certain turbulence strength depends on the density of the fuel (Lisewski et al. 2000; Woosley 2007). To account for this density dependence we consider v' at the flame front in two separate density ranges in simulation I: $(1 < \rho_7 \leq 2)\,10^7\,\mathrm{g\,cm^{-3}}$ and $(2 < \rho_7 \leq 3)\,10^7\,\mathrm{g\,cm^{-3}}$.

The instantaneous maxima of v' in the snapshots of the simulations analyzed here fall around $10^8\,\mathrm{cm\,s^{-1}}$ for all three setups (cf. Tables 2 and 3). They show a similar temporal evolution passing through a peak value. The maxima of v' are slightly lower for less resolved simulations. Since the turbulent subgrid-scale model should compensate for decreasing resolutions, this is not likely due to lower turbulence prediction. Instead, a lower resolution implies a less frequent realization of high turbulence intensities on grid.

3.1. *Probability of high turbulent velocities*

The information gained from determining the maximum turbulent velocities in the simulation is limited since only stochastic realizations are recovered. The robust physical quantity that can be extracted from the simulationss is the probability density function (pdf) of v'. This pdf can be approximated with the normalized histogram of v' determined

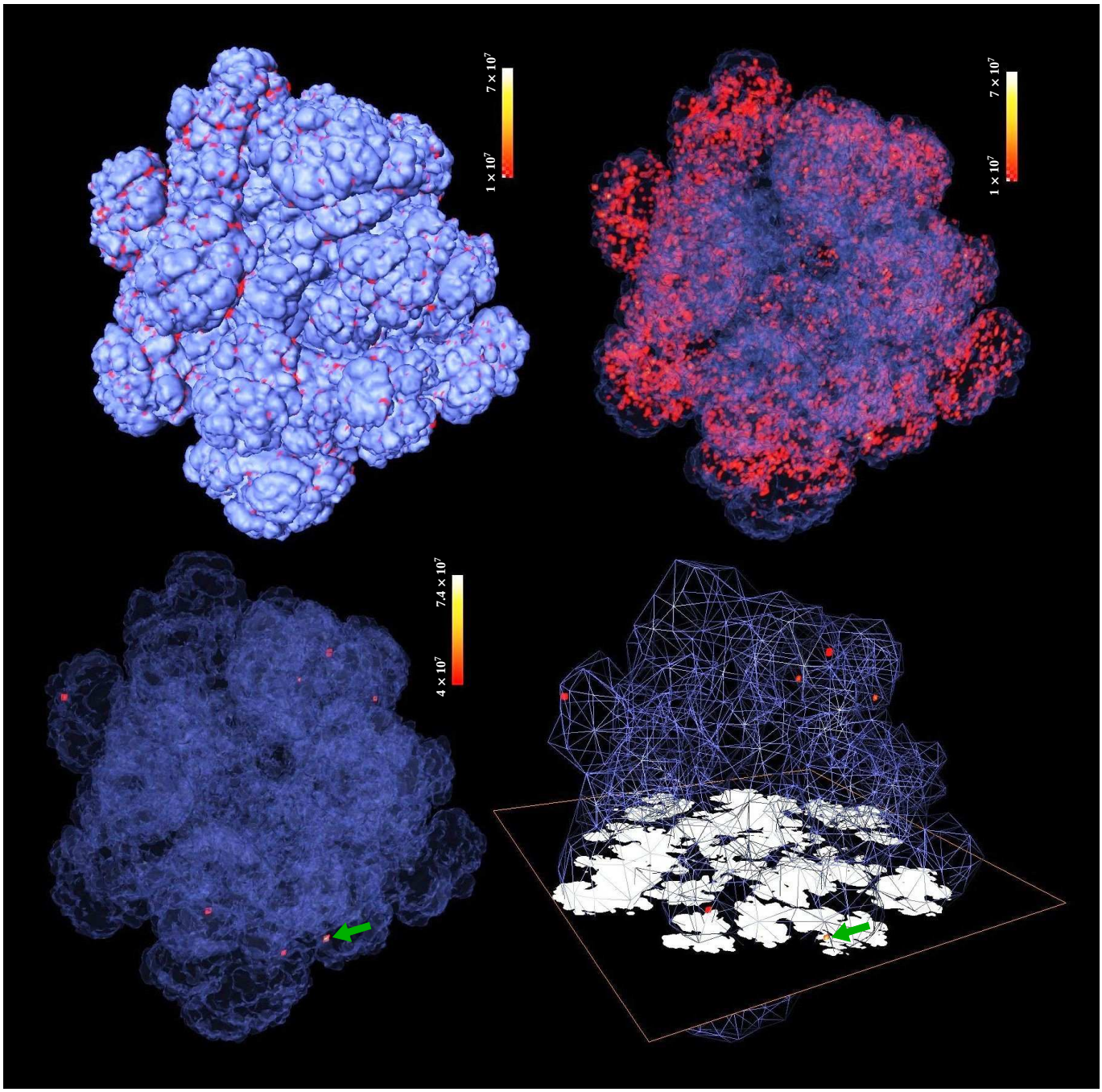

FIG. 2.— Simulation I at $t = 0.80\,\mathrm{s}$ after ignition. The blue opaque, transparent, or wiremesh surfaces correspond to the flame front (implemented via a level-set approach). Volumes of high turbulent velocity fluctuations are rendered in red/orange. In the lower regions, the green arrow indicates the location of the maximum value of v' found in the simulation. For better visibility, white areas correspond to ash regions and fuel regions are shown in black in a plane intersecting with the maximum v'-value in the lower right region.

as described above. An example is shown in Figure 1 *(top)*.

For determining the possibility of detonations, the high-velocity tail is the relevant part of the histogram. An estimate of the corresponding part of the pdf is obtained by fitting the histogram with the exponential of a geometric *Ansatz:*

$$P(v') = \exp\left[a_0 (v')^{a_1} + a_2\right]. \qquad (1)$$

The fit parameters for simulation I at different times are given in Table 2. Integrating this expression from v to ∞ yields the probability of finding v' greater than a given value v,

$$\int_v^\infty P(v')dv' = \frac{v \exp(a_2)\,\Gamma\left(1/a_1, -a_0 v^{a_1}\right)}{a_1 (-a_0)^{1/a_1} v}, \qquad (2)$$

where $\Gamma(.,.)$ denotes the upper incomplete Gamma function. The results of this fitting procedure for an exemplary data set are shown in Figure 1. Obviously, Gaussian or lognormal fits fail to reproduce the high-velocity trend of the histogram (see Fig. 1, *middle*).

Figure 1 *(bottom)* illustrates the time evolution of the probability of finding a turbulent velocity larger than a given value, according to equation (2). At earlier times, the probability of finding $v' \geq 5 \times 10^7\,\mathrm{cm\,s^{-1}}$ is relatively large, but it decreases steeply for higher threshold values. Later on, this decrease flattens out somewhat, but the overall probability becomes lower.

To discuss this behavior, we introduce the probability of finding $v' \geq 10^8\,\mathrm{cm\,s^{-1}}$, $P(10^8)$, because according to Lisewski et al. (2000), this is approximately the threshold for triggering a detonation. Values of $P(10^8)$ are given in Table 2. For simulation I they follow the temporal trend of v'_{max} and decrease steeply towards late times. This evolution might be expected. Turbulence decreases in the late stages of the supernova explosion because the energy injection from buoyancy instabilities becomes lower and due to expansion (the explosion ultimately establishes homologous expansion; Röpke 2005). Thus, the probability of finding high turbulent velocities on any patch of the flame naturally decreases with time. But here we consider only the part of the flame for which the fuel densities are in a certain range. The corresponding flame area increases first and then decreases, since the fuel densities steadily decrease in the explosion process. This area can be estimated from the number of computational cells cut by the flame front and their sizes, providing the value A_{est} given in Tables 2 and 3. This temporal evolution of A_{est} makes realizations of a certain high v' more likely at a particular instant given by the convolution of the area effect with decreasing turbulence strengths. A quantification is provided in Tables 2 and 3 with the size of the flame surface $A_{\mathrm{est}}P(10^8)$ at which $v' > 10^8\,\mathrm{cm\,s^{-1}}$. Obviously, this area needs to exceed a certain size in order to be relevant for a DDT. As seen from Table 2, the evolution of $A_{\mathrm{est}}P(10^8)$ follows the maxima of v' determined at different times in simulation I. However, for the other simulations the trend is less clear. In simulation II the density range of interest is reached later due to lower initial central density. This delays the generation of turbulence and thus burning, energy release, and the expansion of the WD. The overall lower values of $A_{\mathrm{est}}P(10^8)$ derived from simulation II may be taken as an indication that lower central densities decrease the chances of a DDT, but this hypothesis needs to be tested in a larger sample of simulations.

3.2. *Location of high turbulent velocities*

In order to establish a self-sustained detonation wave, a minimum mass of material needs to be burned in the initiation process (Niemeyer & Woosley 1997; Dursi & Timmes 2006; Röpke et al. 2007b). Therefore, it is necessary that the high turbulent velocities are concentrated in larger patches and do not distribute all over the flame in tiny regions. Although $A_{\mathrm{est}}P(10^8)$ exceeds $10^{12}\,\mathrm{cm^2}$ in simulations I and III, there is no guarantee that a connected spatial structure with dimensions larger than 10 km exists. Moreover, the particular location at the flame where the high turbulent velocities are found may be critical for the detonation ignition (Woosley 2007). Do they occur at leading or trailing edges of burning bubbles, or in small channels of fuel in between large ash structures? Such geometrical information cannot be provided by the pdf.

To find answers to these questions we consider the situation at 0.8 s after deflagration ignition in simulation I.

Values of v' exceeding $10^8\,\mathrm{cm\,s^{-1}}$ are directly found in the simulation (see Table 2). The fact that the grid resolution here is $\sim 10^6\,\mathrm{cm}$ indicates that such high turbulent velocities are localized in finite patches. If the area of high turbulent velocity fluctuations determined from the pdf was distributed in many very small patches, it would not be directly visible in the simulation, due to numerical smoothing.

Figure 2 shows the location of the regions of high turbulent intensity at the deflagration flame. The upper left region of Figure 2 demonstrates that flame regions with high turbulent intensities are present mainly at trailing edges of bubble-like structures. The location of all regions with turbulent velocities larger than $10^7\,\mathrm{cm\,s^{-1}}$ is shown again in the upper right region, where the flame has been made transparent in order to make these regions better visible. At the instant shown in Figure 2, the peak value of v' in the analysis of the simulation is found. Its location is illustrated in the lower regions.

3.3. *Possibility of triggering a detonation*

According to Lisewski et al. (2000), values of $v' \gtrsim 10^8\,\mathrm{cm\,s^{-1}}$, corresponding to about 1/5 to 1/4 of the sound speed at the considered densities, are necessary for a DDT (with optimistic assumptions on the DDT mechanism). The exact values depend on the fuel density and composition. For a fuel composition of equal parts, by mass, of carbon and oxygen (this case applies to the simulations analyzed here), a threshold of $v' > 5 \times 10^7\,\mathrm{cm\,s^{-1}}$ is given for a fuel density of $2.3 \times 10^7\,\mathrm{g\,cm^{-3}}$. For lower fuel densities, this threshold becomes larger, and at $8 \times 10^6\,\mathrm{g\,cm^{-3}}$ it is given with $v' > 8 \times 10^7\,\mathrm{cm\,s^{-1}}$. The maxima found in the simulations (in particular, in simulation I; see Tables 2 and 3) exceed these thresholds.

The estimates for the total size of the flame patches where $v' > 10^8\,\mathrm{cm\,s^{-1}}$ and the fact that high values of v' are found at scales resolved in the simulation indicate that the corresponding regions may be sufficiently large to trigger a detonation (compare with the values of detonator sizes given by Niemeyer & Woosley (1997) and Röpke et al. (2007b)).

As noted by Lisewski et al. (2000), the chances of triggering a detonation increase with higher carbon fractions in the fuel and decrease with higher oxygen fractions. Röpke & Hillebrandt (2004) noted that the energy release in burning does not depend strongly on the carbon mass fraction of the fuel as long as it proceeds to nuclear statistical equilibrium. This, however, does not apply to the situation considered here. The low fuel densities imply incomplete burning to intermediate-mass elements. Therefore, in addition to the effect of altering the thresholds of turbulence strength required for triggering a detonation, the carbon mass fraction may also affect the turbulence strength in the distributed burning regime. Additional studies are required to settle this question.

4. CONCLUSIONS

The intensity of turbulence was analyzed at the onset of the distributed burning regime in three-dimensional SN Ia simulations. Considerably larger values for the maximum turbulent velocity fluctuations than previously anticipated (Lisewski et al. 2000) were found for all simulations considered and the conclusion that these values are typical for three-dimensional simulations featuring a state-of-the-art treatment of turbulence on unresolved scales seems compelling. The histogram of v' features a pronounced high-velocity tail. This part is not well fit by a Gaussian pdf but rather by an exponential of a geometric *Ansatz*.

According to our results, a deflagration-to-detonation transition as anticipated by Lisewski et al. (2000) is not ruled out. But, lacking a microphysical model, they cannot provide certainty either, and the concerns pointed out by Niemeyer (1999) persist. However, the results presented here encourage detailed studies of the microphysics of the distributed burning regime at high turbulent velocities, such as those presented by Lisewski et al. (2000) and Woosley (2007).

If a DDT occurs in a SN Ia explosion, then a location at the

outer parts of the deflagration flame, but at the trailing edge of a bubble-like feature, seems most likely. The rapid decline of the pdf towards high turbulence intensities indicates that such a transition may be a rare event, possibly realized only once or a few times in a supernova. This, however, as well as the question of whether a DDT occurs in every event, depends on the details of the formation of the detonation and warrants further study.

It may thus be possible that detonations do not form at all leading features of deflagration flame but only in a few such locations. As a detonation front cannot cross even tiny regions filled with nuclear ash (Maier & Niemeyer 2006), it may not reach all patches of unburnt material embedded in the complex deflagration structure. However, in numerical simulations of delayed detonations in WD with parametrized DDTs, Röpke & Niemeyer (2007) found that even a detonation front formed in a single spot burns most of the remaining fuel by reaching the dense center of the star. Such large-scale supernova simulations with parametrized DDTs help to address the question of whether the outcome of delayed detonations is consistent with observational data (Mazzali et al. 2007).

Stan Woosley greatly supported this work with stimulating discussions. The simulations have been performed on facilities of the Max Planck Society, Garching, Germany, the HPCx, Edinburgh, UK (as part of the DEISA project), and at the National Center for Computational Sciences at Oak Ridge National Laboratory, which is supported by the Office of Science of the U.S. Department of Energy, under contract DE-AC05-00OR22725. The work was supported by the SciDAC Program of the DOE (DE-FC02-01ER41176) and the NASA theory program (NNG 05-GG08G).

REFERENCES

Arnett, W. D. 1969, Ap&SS, 5, 180
Dursi, L. J., & Timmes, F. X. 2006, ApJ, 641, 1071
Gamezo, V. N., Khokhlov, A. M., Oran, E. S., Chtchelkanova, A. Y., & Rosenberg, R. O. 2003, Science, 299, 77
Khokhlov, A. M. 1991, A&A, 245, 114
Kozma, C., Fransson, C., Hillebrandt, W., Travaglio, C., Sollerman, J., Reinecke, M., Röpke, F. K., & Spyromilio, J. 2005, A&A, 437, 983
Lisewski, A. M., Hillebrandt, W., & Woosley, S. E. 2000, ApJ, 538, 831
Maier, A., & Niemeyer, J. C. 2006, A&A, 451, 207
Mazzali, P. A., Röpke, F. K., Benetti, S., & Hillebrandt, W. 2007, Science, 315, 825
Niemeyer, J. C. 1999, ApJ, 523, L57
Niemeyer, J. C., & Kerstein, A. R. 1997, New Astronomy, 2, 239
Niemeyer, J. C., & Woosley, S. E. 1997, ApJ, 475, 740
Reinecke, M., Hillebrandt, W., & Niemeyer, J. C. 2002a, A&A, 386, 936
—. 2002b, A&A, 391, 1167
Reinecke, M., Hillebrandt, W., Niemeyer, J. C., Klein, R., & Gröbl, A. 1999, A&A, 347, 724
Röpke, F. K. 2005, A&A, 432, 969
Röpke, F. K., & Hillebrandt, W. 2004, A&A, 420, L1
—. 2005, A&A, 431, 635
Röpke, F. K., Hillebrandt, W., Niemeyer, J. C., & Woosley, S. E. 2006, A&A, 448, 1
Röpke, F. K., Hillebrandt, W., Schmidt, W., Niemeyer, J. C., Blinnikov, S. I., & Mazzali, P. A. 2007a, ApJ, 668, 1132
Röpke, F. K., & Niemeyer, J. C. 2007, A&A, 464, 683
Röpke, F. K., Woosley, S. E., & Hillebrandt, W. 2007b, ApJ, 660, 1344
Schmidt, W., Niemeyer, J. C., Hillebrandt, W., & Röpke, F. K. 2006, A&A, 450, 283
Timmes, F. X., & Woosley, S. E. 1992, ApJ, 396
Woosley, S. E. 2007, ApJ, 668, 1109
Zingale, M., Woosley, S. E., Rendleman, C. A., Day, M. S., & Bell, J. B. 2005, ApJ, 632, 1021